http://dx.doi.org/10.15576/GLL/2021.2.7

GLL

Geomatics, Landmanagement and Landscape No. 2 • 2021, 7–21

TWO METHODS TO MITIGATE INSAR-BASED DEMS VEGETATION IMPENETRABILITY BIAS

Sławomir Tulski, Kazimierz Bęcek

Summary

Digital elevation models (DEM), including the Shuttle Radar Topography Mission (SRTM), are used in many branches of geoscience as an ultimate dataset representing our planet's surface, making it possible to investigate processes that are shaping our world. The SRTM model exhibits elevation bias or systematic error over forests and vegetated areas due to the microwaves' peculiar properties that penetrate the vegetation layer to a certain depth. Numerous investigations identified that the penetration depth depends on the forest density and height. In this contribution, two methods are proposed to remove the impact of the vegetation impenetrability effect. The first method is founded on the multiple regression of two forest characteristics, namely forest height and forest density. The second method uses a lookup table approach. The lookup table and the multiple regression explanatory variables are taken from the freely available datasets, including the forest density data (MODIS_VCF) and global tree height map (GTHM). An important role in this research is played by the Ice, Clouds, and Land Elevation Satellite (ICESat) data. The accuracy tests indicate that the first method eliminates approximately 68% of the elevation bias, while the second method appears to be more effective, leading to almost complete removal of the vegetation bias from the SRTM data. The methods are fine-tuned to the local coniferous forests in Poland. Additional studies are required to fine-tune the methods for the leaf-off state of deciduous forests. However, a new set of parameters for both methods can be quickly developed for different locations and forest types. Both methods' functionality and effectiveness can be improved once more accurate forest tree height and vegetation density data become available. These methods are universal in mitigating the vegetation bias from the Synthetic Aperture Radar Interferometry (InSAR) derived model and photogrammetric models.

Keywords

SRTM • vegetation bias • impenetrability • ICESat • GTHM

1. Introduction

Digital Elevation Models (DEM) – a digital way to represent the topography of Earth – are nowadays a commonly used data type in many branches of geosciences [e.g., Wright et al. 2006, Bailey et al. 2007, Berthier et al. 2007, Becek 2011, Baugh et al.

2013], and also in the mitigation of natural and anthropogenic hazards and catastrophic events, spatial planning and other fields of human activities [Vassilopoulou and Hurni 2001, Foruko and Tsawo 2013]. DEMs are developed from various surveys, including *in situ* measurements and digital photographs (photogrammetry). A significant leap in surveying technology has been achieved thanks to the Synthetic Aperture Radar Interferometry (InSAR) and advances in satellite-based sensors. An essential benefit of the satellite-based InSAR method is their regional to global extent. At the turn of the millennium in 2000, thanks to the Shuttle Radar Topography Mission (SRTM), a global DEM has been developed, which is free to use for everyone [Rodríguez et al. 2006, JPL 2021]. A considerable limitation of InSAR-based DEMs is an effect known as the vegetation impenetrability bias [Becek 2011]. The effect is due to the limited penetrability of microwaves of vegetation.

Consequently, InSAR elevation over the vegetation-covered area is always overestimated. The magnitude of the bias depends, among other things, on the height of trees and forest density. We should note that the impenetrability effect benefits some branches of science because, among other things, it facilitates vegetation studies [Becek 2008b]. Several researchers developed methods to mitigate the vegetation bias [e.g., Wilson et al. 2007, Paiva et al. 2011, Baugh et al. 2013, Su and Guo 2014]. However, the solutions they proposed had been prepared for specific locations and applications (hydrology studies). In the present paper, we outline two methods to minimize the impact of vegetation bias. According to our tests, the proposed methods offer a better universality than the other methods offered elsewhere. An important limitation to the study is that the methods' parameters were determined for forests in Poland. However, the parameters for new locations can be quickly established, using this paper as a guide.

2. Materials and methods

The present study was carried out using various data types, including ICESat, SRTM, Corine Land Cover 2000, European Tree Species Map, Global Tree Height Map, MODIS Vegetation Continuous Field (MODIS_VCF), and SRTM. In the following section of the paper, we shortly summarise these remotely sensed and freely available datasets.

2.1. ICESat Data

ICESat is a concluded satellite mission that is currently followed by the ICESat-2 program. The ICESat missions' objectives include monitoring the topography icefields [DiMarzio 2007, Zwally et al. 2011], land topography measurements [Beaulieu and Clavet 2009, Carabajal 2011], vertical structure, horizontal distribution of clouds [Zwally et al. 2002], and vegetation studies [Simard et al. 2008, Simard et al. 2011, Hayashi et al. 2013]. ICESat satellite conducted its mission between 2003–2010. It was a segment of the Earth Observation Program (EOS) [Schutz et al. 2005] developed by the National Aeronautics and Space Agency (NASA). The ICESat operated from

a circular orbit, 600 km above sea level, and conducted monitoring Earth's surface between 86°N and 86°S.

The main instrument of the ICESat satellite was Geoscience Laser Altimeter System (GLAS). The instrument was the first known case of using a laser to monitor Earth's surface and atmosphere, installed as a civilian satellite. The laser used two bands: infrared (1064 nm) and green (532 nm), and short pulses of energy with 40 Hz frequency. An approximate footprint of the laser spot on Earth's surface was 70 m, and an average distance between the subsequent spots was 172 m [Abshire et al. 2005]. The elevation readings were referred to the TOPEX/Poseidon ellipsoid. The GLAS instrument was of the *full-waveform* form. This type of Lidar instrument allows for enhanced analysis of the Lidar beam's intercepts representing elements of the land cover's vertical structure, e.g., vegetation [Chen 2010a, Brenner et al. 2011]. The ICESat data are available at several processing levels. In this project, the GLAH14 version 33 was used. According to some researchers, the ICESat elevations' horizontal/vertical accuracy is 5 to 15 m and 1 to 10 m, respectively [Doung et al. 2009, Shtain and Filin 2011, Tulski 2014].

2.2. SRTM data

The Space Shuttle Topography Mission (SRTM) was designed to collect data for the production of semi-global (56°S to 60°N) DEM covering 80% of Earth's landmasses during an 11-day flight in February 2000 [Farr et al. 2007]. SRTM data have been used by researchers in many branches of geosciences, including geomorphology [Bailey et al. 2007], hydrology [Baugh et al. 2013], vulcanology [Wright et al. 2006], glaciology [Berthier et al. 2007], vegetation studies [Kellndorfer et al. 2004], and forest biomass studies [Becek 2011]. SRTM data at three arcsec spatial resolution are used in this study. Elevation of SRTM is referenced to EGM96 geoid. Extensive studies of the vertical accuracy of SRTM data confirmed that the real accuracy was significantly higher as assumed by the project's design [Rodríguez et al. 2006, Berry et al. 2007, Becek 2006, 2008a, 2014] SRTM is described in the literature as a DEM. However, as an InSAR method's product, it suffers from vegetation bias over vegetated areas. The vegetation bias magnitude is related to vegetation height [Carabajal and Harding 2006] and vegetation density [Becek 2008b]. The vegetation impenetrability is approximately 70–80% for a natural and fully stocked forest [Becek 2006].

2.3. Global Tree Height Map (GTHM)

The vegetation impenetrability effect allows for the estimation of forest height. Two attempts to create a global tree height map were made by Lefsky [2010] and Simard et al. [2011]. According to studies [Simard et al. 2011, Bolton et al. 2013], the latter GTHM is more accurate. Hence the latter GTHM is used in this project. The GTHM was developed based on SRTM data. The spatial resolution of the model is 1 km × 1 km. The model is distributed together with an accuracy map.

2.4. MODIS Vegetation Continuous Fields (MODIS_VCF)

A Moderate-resolution Imaging Spectroradiometer (MODIS) instrument installed on the Terra satellite produced several vegetation-related datasets, including the MODIS_VCF dataset. The MODIS_VCF contains a raster called PPR that represents the fraction of pixels covered by trees. The spatial resolution of the PPR is 250 m × 250 m (Townshend et al., 2011.)

2.5. Corine Land Cover 2000 (CLC2000)

The CLC2000 is a dataset created by the European Environment Agency (EEA) concerning 32 European countries' land cover. The CLC2000 was developed from the Landsat ETM data that were acquired between 1999 and 2000. There are 44 classes of land cover, including a forest layer. The dataset is at 100 m × 100 m spatial resolution and is available in both a raster and vector format. The CLC2000 dataset was used in this project to select forest areas for testing purposes.

2.6. Tree species maps for Europe (EU_TSM)

The EU_TSM developed by EFI (European Forest Institute) and Alterra/Wageningen University and Research Centre (Brus et al., 2011.) The dataset represents the spatial distribution of the common twenty types of tree species in Europe. A 1 km × 1 km pixel represents a dominant tree species. This project used the dataset to determine the dominant tree species of forest complexes selected for testing purposes.

3. Methods

3.1. Initial processing of ICESat data

The ICESat data were initially pre-processed to remove outliers. The following parameters available in the metadata file were used to eliminate outliers:

- *elev_use_flag* = 0 (valid data tag),
- *sat_corr_flg* = 0 (saturation tag),
- *FRir_qa_flg* = 15 (cloud-free shot), and
- *d_elev* elevation should not differ from the corresponding elevation by more than *abs* (25 m).

In the next step, three elevations were extracted from the ICESat data for each laser shot. The first one –*d_elev*– represents the center of the reflected laser pulse. The –*d_elev*– elevation is equivalent to DSM elevation; over vegetated areas, it is close to SRTM elevations [Carabajal and Harding 2006].

The second elevation used is the elevation of terrain (ICE_{DTM}), and the third one was the elevation of the vegetation canopy (ICE_{can})

Subtracting ICE_{DTM} and ICE_{can} yields the tree height (ICE_t) (1):

$$ICE_t = ICE_{can} - ICE_{DTM} \tag{1}$$

ICESat elevations were converted from the Topex/Poseidon to the EGM08 geoid using the metadata-delivered *d_gdHt* correction. Conversion from EGM08 to EGM96 was neglected as insignificant given the other error source [Trojanowicz 2009].

3.2. Dependency of the impenetrability on the vegetation density

The magnitude of the impenetrability depends on the vegetation density [Becek 2008b]. The higher the vegetation density or vegetation cover percentage of a given unit area, the higher the impenetrability. The correlation appears to be a linear one. The latter statement was tested on forests located in Poland. The tests were carried out over both coniferous and deciduous forests using 15906 and 2842 ICESat laser shots for the former and latter types of forest. The dominant tree species were Baltic pine (*Pinus sylvestris* L.), birch (*Betula* L.), common oak (*Quercus robur* L.), and Alnus (*Alnus* L.) Note that SRTM data were collected during the leaf-off state, implying a lower impenetrability magnitude for the deciduous forest.

For each laser shot, using MODIS_VCF, the vegetation density was estimated, and the vegetation impenetrability was calculated from (2):

$$IMP_C = SRTM - ICE_{DTM} \tag{2}$$

where:

IMP_C – impenetrability,
$SRTM$ – SRTM elevation,
ICE_{DTM} – ICESat ground elevation.

3.3. Dependency of impenetrability on vegetation height

According to Carabajal and Harding [2006], the magnitude of impenetrability depends on vegetation height. This conclusion is trivial, knowing that the phase center (reflection) of microwaves is located within the vegetation's canopy. Hence, higher vegetation causes a larger magnitude. The conclusion results from the analysis of the *wfExt* (ICESat) readings that represent the laser reflection duration and differences SRTM *minus* ICESat (IMP_C). However, *wfExt* is also too high in hilly terrain. This is because the returning reflection's end represents the lowest fragment of the ground hit by a laser shot. In this project, vegetation height was estimated using (1) and the impenetrability using (2) to avoid the effect.

3.4. Estimation of vegetation impenetrability

Several authors have investigated the estimation of vegetation impenetrability but without finding a universal solution. Paiva and co-authors [Paiva et al. 2011] proposed the use of an external data source for tree heights for a given area. Tree height is a spatial, temporal, and species-dependent variable. The major problem with this approach is the availability of suitable reference data. A similar approach using Lidar data is costly and does not offer a universal solution [Su and Guo 2014]. The method proposed by Wilson and co-authors [Wilson et al. 2007] is about subtracting half of the tree heights estimated from local reference data. Following the same idea, Baugh and co-authors [Baugh et al. 2013] proposed to use global tree height reference data (GTHM). The experiment was conducted over Amazonia. SRTM data were modified by subtracting quantiles of the GTHM tree heights until resulting elevations were similar to a high-resolution reference elevation.

3.5. A proposal for two new methods for estimating vegetation impenetrability

In the following section, two new methods for estimating the vegetation impenetrability are proposed and tested. The first method, named the *gTree_norm* method, is constructed on multiple regression of two explanatory variables, i.e., forest height and forest density. The forest height/density (or vegetation height/density) is derived from ICESat and MODIS_VCF freely available data.

The second method, termed the *gTree_tuned* method, mitigates a low accuracy of GTHM data [Bolton et al. 2013] and its weak correlation with the ICESat estimated tree heights (ICE_t) (Fig. 3–5).

First, the ICESat data were grouped into few classes by the vegetation density and vegetation height. Three vegetation density classes according to MODIS_VCF data were selected (%): (50–60), (60.1–70), (70.1–80), and ten classes of tree heights according to GTHM data (m): (14–15), (15.1–16), (16.1–17), (17.1–18), (18.1–19), (19.1–20), (20.1–21), (21.1–22), (22.1–23), (23.1–24).

In the next step, a median of IMP_C for each class was used to identify correlations with GTHM. The method was tested on selected forest plots in Poland of approx. 1.3 km² (range 0.8 km² to 2.4 km²) in size. Each plot received at least five ICESat shots, with the average of 13 shots. There were 333 plots considered in the tests. For each plot, an average forest height (GTHM), average forest density (MODIS_VCF), and the impenetrability IMP_C were calculated. As reference impenetrability, a weighted impenetrability $wIMP_C$ was calculated according to the following procedure:

1. Average terrain slope *s* within each ICESat footprint from SRTM was calculated.
2. Average impenetrability IMP_C for each footprint was calculated from (2).
3. Weighted average impenetrability $wIMP_C$ for each test plot was calculated using (3) and (4):

$$wIMP_C = \frac{\sum \left(IMP_C\right)_j^i * w_i}{\sum w_i};\ i = 1, ..., n;\ j = 1, ..., k \tag{3}$$

$$w = \begin{Bmatrix} 10\ for\ s = 0^\circ \\ 0\ for\ IMP_C < 0 \\ \dfrac{12}{q^2\ tan^2\ (s)}\ for\ s > 0^\circ \end{Bmatrix} \tag{4}$$

where:

$wIMP_C$ – weighted average impenetrability,
w – weight,
k – number of laser shots within a test plot,
n – number of test plot,
s – average terrain slope within a pixel,
q – diameter of laser footprint (approx. 70 m²).

Weighted impenetrability controls the impact of measurement noise, including terrain's slope and pixel size. For flat terrain ($s = 0°$), the weight is 10. For $IMP_C < 0$, the measurement is neglected. For $s > 0°$, the weight follows a reciprocal of the elevation error in any DEM caused by the slope and pixel size [Becek 2008a, 2011, 2014]. For example, the weight for $s = 1°$ is 8.04 and drops fast for higher slopes.

4. Results

4.1. Vegetation density

Figure 1 shows a comparison between impenetrability of vegetation (IMP_C) vs. vegetation density for coniferous (left pane) and deciduous forest (right pane). Despite a considerable noise due to, among other things, a low resolution of the vegetation density data (MODIS_VCF), a trend is recognizable. However, the relationship is too weak to estimate the impenetrability magnitude reasonably well. Another point is that vegetation density must be considered as one of the vegetation impenetrability explanatory variables. It is interesting to note that Figure 1 reveals a systematic error of SRTM, i.e., elevations are too low by approx. 3 m, which is visible for vegetation density 0–10%. This result is consistent with the reported magnitude of the error at 1.67 m and 3.7 m in [Becek 2014] and [Karwel and Ewiak 2008], respectively.

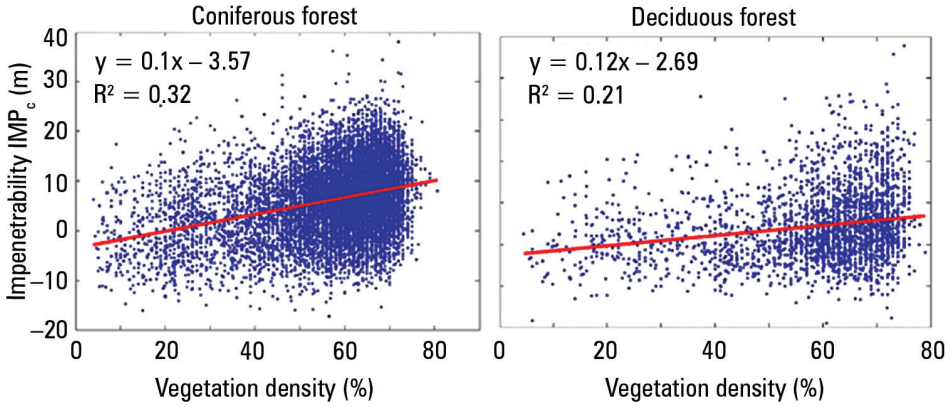

Fig. 1. Comparison between impenetrability vs. vegetation density for coniferous forest (left pane) and deciduous forest (right pane)

4.2. Impenetrability vs. vegetation height

A summary of the comparison between the impenetrability vs. tree height is presented in Table 1 and Figure 2. The mean deciduous forest's impenetrability is lower than for coniferous forest, which is understandable because of the leaf-off state of trees in Winter. Note that mean impenetrability, 32% and 23% for coniferous and deciduous forests, respectively, is lower than reported by some authors [Sexton et al. 2009, Becek 2011]. According to Chen [2010b], this is caused by the overestimation of tree heights in ICESat data.

Table 1. Mean impenetrability for forest types

	Coniferous forest	Deciduous forest
Mean forest height (m)	20.1	20.2
Mean impenetrability (m)	6.5	4.7
Mean impenetrability (%)	32	23

Figure 2 shows a regression line that models a relationship between the vegetation impenetrability IMP_C and coniferous forest height (left pane) and deciduous forest height (right pane). In both cases, correlation coefficient R^2 is approx. 0.7. These regression parameters are subject to forest density.

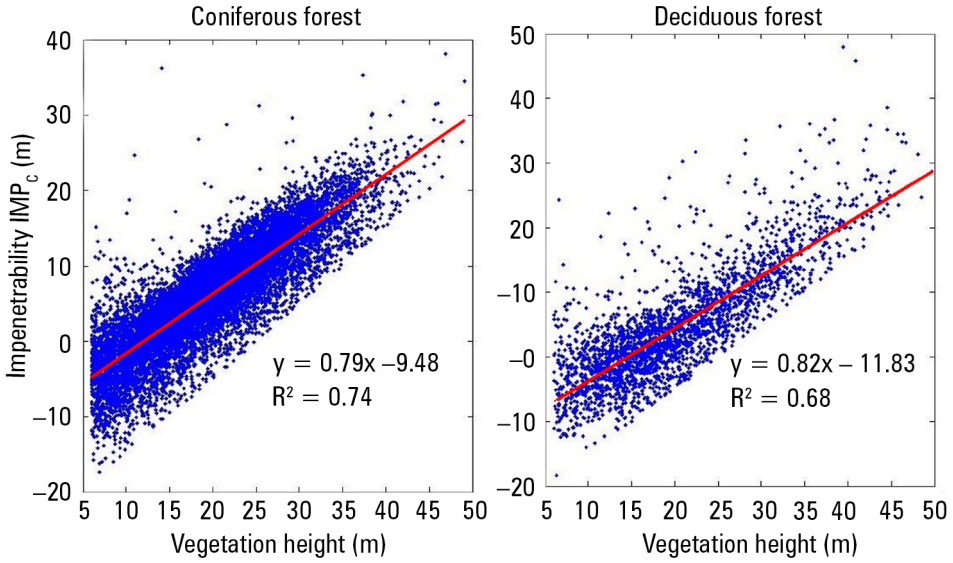

Fig. 2. Correlation between impenetrability vs. forest height for coniferous forest (left pane) and deciduous forest (right pane)

4.3. Correcting SRTM for the impenetrability

4.3.1. Application of the *gTree_norm* method

Table 2 shows the explanatory variable's multiple regression, i.e., forest height and forest density against IMP_C, for both types of trees, coniferous and deciduous. The correlation coefficient R^2 indicates that the correlation is strong. In Table 4, an accuracy assessment of the vegetation impenetrability is shown.

The method is capable of eliminating approx. 68% of the impenetrability from the SRTM data. Considering the low spatial resolution of vegetation density data (MODIS_VCF) and tree height (GTHM), the result is satisfactory. The average difference between the actual IMP_C and the figure estimated from the regression model is 2.68 m with a standard deviation of 3.34 m. The accuracy of the IMP_C determination mainly depends on the accuracy of GTHM. The accuracy will increase when the tree height model is of higher resolution and accuracy.

Table 2. The *gTree_norm* method summary

Forest type	Model	R^2
Coniferous forest	$IMP_C = 0.76h + 0.08d - 13.35$	0.76
Deciduous forest*	$IMP_C = 0.81h + 0.04d - 13.80$	0.68
where h and d are mean forest height (m) and density (%)		

4.3.2. Application of the *gTree_tuned* method

Figure 3 shows a correlation between impenetrability vs. tree height (GTHM) for three classes of forest density MODIS_VCF. The regression lines (equations are presented in Figure 3) for each forest density class are very similar, suggesting that the forest density's impact on the impenetrability is relatively small, at least for densities > 50%. A lookup table is more convenient to use than a graph .

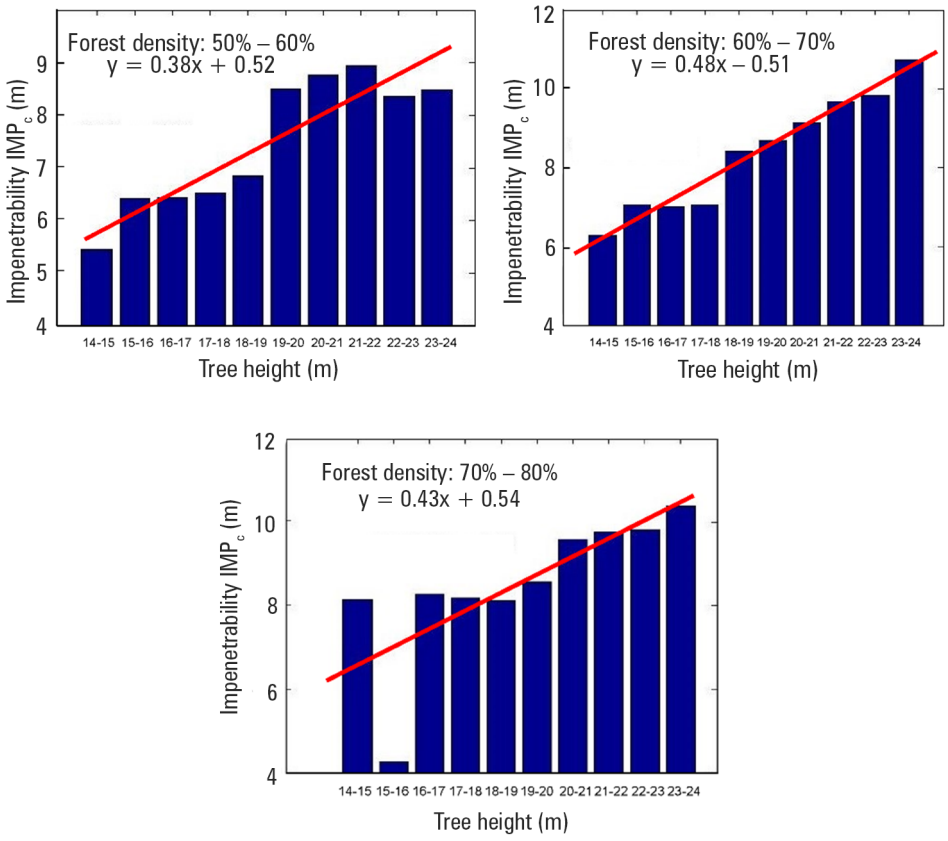

Fig. 3. Correlation between impenetrability IMP_C vs. GTHM derived forest height class for 50–80% of vegetation density

Table 3 is a lookup table helping the potential user estimate the elevation bias or the vegetation impenetrability over coniferous forests. The data are optimized for the forests located in the territory of Poland. The lookup table can be implemented as a computer or web application for easy reference or corrections of the SRTM data. Similarly, the gTree_norm method can be enabled in the same way. It should be stressed that neither methods has been validated over the deciduous forest stands. Additional studies are required to fine-tune the methods for the leaf-off status of forest stands.

Table 3. A lookup table of forest impenetrability as a function of forest height and forest density

Forest height (m)	Vegetation density		
	50–60%	61–70%	71–80%
	Forest impenetrability (m)		
14	5.85	6.21	6.56
15	6.23	6.69	6.99
16	6.61	7.17	7.42
17	6.99	7.65	7.85
18	7.37	8.13	8.28
19	7.75	8.61	8.71
20	8.13	9.09	9.14
21	8.51	9.57	9.57
22	8.89	10.05	10.00
23	9.27	10.53	10.43

4.3.3. Accuracy assessment of the impenetrability compensating methods

Table 4 summarises accuracy tests for the *gTree_norm* and *gTree_tuned* methods. According to the tests, the average difference between the IMP_C obtained from the *gTree_norm* model, and the average IMP_C values for the test forest stands is 2.68 m with a standard deviation of 3.34 m. However, in the *gTree_tuned* method, the difference is 0.2 m with a standard deviation of 3.12 m. This observation appears to promote the *gTree_tuned* method.

Table 4. Accuracy assessment of impenetrability (IMP_C) for *gTree_norm* and *gTree_tuned* methods

	gTree_norm	gTree_tuned			
		Forest density			Average (m)
		50–60%	60.1–70%	70.1–80%	
Average IMP_C (m)	8.52	7.45	8.84	10.1	8.52
Model IMP_C (m)	5.84	7.17	8.85	9.23	8.32
Difference (m)	2.68	0.28	0.01	0.87	0.20
STD (m)	3.34	3.03	3.28	2.46	3.12

4.3.4. Postscriptum

This study was conducted several years ago using the data available at the time, including ICESat, MODIS_VCF data. Over the last seven or so years, new data sets were generated, relevant for the study, including the Global Forest Canopy Height map (GFCH) [Potapov et al. 2020], AW3D30 m, a global digital elevation model developed from optical stereo images [Tadono et al. 2014], Lidar-based DTM model [Geoportal 2021], and are now freely available. Hence, having new data sets, it is possible to conduct a similar study as the one here presented. We want to encourage readers to embark on a venture to verify and improve the findings presented in this article. The InSAR technology is a powerful method for producing DEMs and other products, including terrain deformation. Hence, for the foreseeable future, we will see new InSAR-based products emerging with all their shortcomings, including the vegetation impenetrability, which justifies studies like this.

5. Conclusions

This study concerning vegetation impenetrability mitigation caused by limited vegetation transparency to microwaves introduces two methods to resolve the SRTM digital elevation data product issue. A careful and comprehensive assessment of the methods allows formulating the following conclusions.

1. The *gTree_norm* method, based on the multi regression of forest height and density, was parametrized for the coniferous forest (pine trees). Caution must be exercised using the deciduous forest parameters because this type of forest's impenetrability is valid for the leaf-off status only (SRTM was flown in Winter). A new set of parameters must be established for other world regions or different tree species. It is estimated that an estimated 60% of the impenetrability bias can be removed using this method. More accurate results can be expected if the GTHM and MODIS_VCF data were replaced with higher resolution datasets.
2. The *gTree_tuned* method can be used in the case no other than GTHM, and MODIS_VCF data are onhand because, as the method's validation indicates, almost the entire impenetrability bias is removed.
3. Both methods are universal in terms of the world's location and spatial scale. The methods can mitigate the impenetrability error, extending the SRTM data's applicability for forested areas covering some 30% of the world's landmass.
4. New data sets are currently available that are suitable for similar studies. Readers are encouraged to facilitate similar projects.

References

Abshire J.B., Sun X., Riris H., Sirota J.M., McGarry J.F., Palm S., Yi D., Liiva P. 2005. Geoscience Laser Altimeter System (GLAS) on the ICESat Mission: On-orbit measurement performance. Geophys. Res. Lett., 32(21).

Bailey J.E., Self S., Wooller K., Mouginis-Mark P.J. 2007. Discrimination of fluvial and eolian features on large ignimbrite sheets around La Pacana Caldera, Chile, using Landsat and SRTM-derived DEM. Rem. Sens. Env., 108(1), 24–41.

Baugh C.A., Bates P.D., Schumann G., Trigg M.A. 2013. SRTM vegetation removal and hydrodynamic modeling accuracy. Water Res. Res., 49, 5276–5289.

Beaulieu A., Clavet D. 2009. Accuracy Assessment of Canadian Digital Elevation Data Using ICESat. Photogramm. Rem. Sens., 75(1), 81–86.

Becek K. 2006. Accuracy Evaluation of the SRTM Topographic Data Product over Selected Sites in Australia and Brunei Darussalam. Rep. Geodesy, 77(2), 283–289.

Becek K. 2008a. Investigating error structure of shuttle radar topography mission elevation data product. Geophys. Res. Lett., 35(15), L1540.

Becek K. 2008b. Investigation of Elevation Bias of the SRTM C and X Band Digital Elevation Models. Int. Arch. Photogram. Rem. Sens. Spat. Inf. Sci., XXXVII (B1).

Becek K. 2011. Biomass Representation in Synthetic Aperture Radar Data Sets: A comprehensive study of biomass-induced elevation bias in DEMs derived using Synthetic Aperture Radar Interferometry. http://www.amazon.com/Biomass-Representation-Synthetic-Aperture Radar/dp/3844323422/ref=sr_1_1?s=books&ie=UTF8&qid=1397435185&sr=1-1 (accessed: 6.02.2021).

Becek K. 2014. Assessing Global Digital Elevation Models Using the Runway Method: The Advanced Spaceborne Thermal Emission and Reflection Radiometer Versus the Shuttle Radar. IEEE Trans. Geosc. Rem. Sens., 54(8) 4823–4831.

Berry P.A.M., Garlick J.D., Smith R.G. 2007. Near-global validation of the SRTM DEM using satellite radar altimetry. Rem. Sens. Envir., 106(1), 17–27.

Berthier E., Arnaud Y., Kumar R., Ahmad S., Wagnon P., Chevallier P. 2007. Remote sensing estimates of glacier mass balances in the Himachal Pradesh, Western Himalaya, India. Rem. Sens. Env., 108(3), 327–338.

Bolton D.K., Coops N.C., Wulder M.A. 2013. Investigating the agreement between global canopy height maps and airborne Lidar derived height estimates over Canada. Can. J. Rem. Sens., 39(S1), S139–S151.

Brenner A.C., Zwally H.J., Bentley C.R., Csatho B.M., Harding D.J., Hofton M.A., Minster J. B., Roberts L.A., Saba J.L., Thomas R.H., Yi D. 2011. Geoscience laser altimeter system algorithm theoretical basis document: Derivation of range and range distributions from laser pulse waveform analysis. Algorithm Theoretical Basis Documents (ATBD). www.csr.utexas.edu/glas/atbd.html (accessed: October 2014).

Brus D.J., Hengeveld G.M., Walvoort D.J.J., Goedhart P.W.A., Heidema H., Nabuurs G.J., Gunia K. 2011. Statistical mapping of tree species over Europe. Euro. Journ. Forest Res., 131(1), 145–157.

Carabajal C.C, Harding D.J. 2006. SRTM C-Band and ICESat Laser Altimetry Elevation Comparisons as Function of Tree Cover and Relief. Photogramm. Eng. Rem. Sens., 72(3), 287––298.

Carabajal C.C. 2011. ASTER Global DEM ver. 2.0 evaluation using ICESat geodetic ground control. ICESat/GSFC Validation Report. http://www.jspacesystems.or.jp/ersdac/GDEM/ver2Validation/Appendix_D_ICESat_GDEM2_validation_report.pdf (accessed: October 2014).

Chen Q. 2010a. Assessment of terrain elevation derived from satellite laser altimetry over mountainous forest areas using airborne Lidar data. ISPRS Photogramm. Rem. Sens., 65, 111–122.

Chen Q. 2010b. Retrieving vegetation height of forests and woodlands over mountainous areas in the Pacific Coast region using satellite laser altimetry. Rem. Sens. Env., 114, 1610–1627.

DiMarzio J.P. 2007. GLAS/ICESat 1 km Laser Altimetry Digital Elevation Model of Greenland. Boulder, Colorado USA: National Snow and Ice Data Center.

Doung H.R., Lindenberghm Pfeifer N., Vosselman G. 2009. ICESat Full-Waveform Altimetry Compared to Airborne Laser Scanning Altimetry Over The Netherlands. *IEEE Trans. Geosci. Rem. Sens.,* 7(10) 3365–3378.

EEA. Corine Land Cover 2000 seamless vector data. https://www.eea.europa.eu/data-and-maps/data/clc-2000-vector-6 (accessed: 6.02.2021).

Farr T.G., Rosen P.A., Caro E., Crippen R., Duren R., Hensley S., Kobrick M., Paller M., Rodriguez E., Roth L., Seal D., Shaffer S., Shimada J., Umland J., Werner M., Oskin M., Burbank D., Alsdorf D. 2007. The Shuttle Radar Topography Mission. Rev. Geophys., 45(2).

Forkuo E.K., Tsawo V.A. 2013. The use of digital elevation models for water-shed and flood hazard mapping. Int. J. Rem. Sens. Geosc., 2(2), 56–65.

Fricker H.A., Borsa A., Minster B., Carabajal C.C., Quinn K., Bills B. 2005. Assessment of ICESat performance at the Salar de Uyuni, Bolivia. Geophys. Res. Lett., 32(21).

Geoportal. 2021. Numeryczne modele wysokościowe. https://www.geoportal.gov.pl/dane/numeryczne-modele-wysokosciowe (accessed: 6.02.2021).

Hayashi M., Saigusa N., Oguma H., Yamagata Y. 2013. Forest canopy height estimation using ICESat/GLAS data and error factor analysis in Hokkaido, Japan. ISPRS J. Photogramm. Rem. Sens., 81, 12–18.

JPL 2021. Shuttle Radar Topography Mission. http://www2.jpl.nasa.gov/srtm/ (accessed: 6.02.2021).

Karwel A.K., Ewiak I. 2008. Estimation of the accuracy of the SRTM terrain model on area of Poland. Int. Arch. Photogramm. Rem. Sens. Spat. Inf. Sci., XXXVII(B7).

Kellndorfer J., Walker W., Pierce L., Dobson C., Fites J.A., Hunsaker C., Vona J., Clutter M. 2004. Vegetation height estimation from Shuttle Radar Topography Mission and national elevation datasets. Rem. Sens. Env., 93(3), 339–358.

Lefsky M.A. 2010. A global forest canopy height map from the Moderate Resolution Imaging Spectroradiometer and the Geoscience Laser Altimeter System. Geophys. Res. Lett., 37(15).

Paiva R.C.D., Collischonn W., Tucci C.E.M. 2011. Large scale hydrologic and hydrodynamic modeling using limited data and a GIS based approach. J. Hydr., 406, 170–181.

Potapov P., Li X., Hernandez-Serna A., Tyukavina A., Hansen M.C., Kommareddy A., Pickens A., Turubanova S., Tang H., Silva C.E., Armston J., Dubayah R., Blair J.B., Hofton M. 2020. Mapping and monitoring global forest canopy height through integration of GEDI and Landsat data. Rem. Sens. Env., 253, 112165.

Rodríguez E., Morris C.S., Belz J.E. 2006. A Global Assessment of the SRTM Performance. Photogramm. Eng. Rem. Sens., 72(3), 249–260.

Schutz B.E., Zwally H.J., Shuman C.A., Hancock D., DiMarzio J.P. 2005. Overview of the ICESat Mission. Geophys. Res. Lett., 32(21).

Sexton J.O., Bax T., Siqueira P., Swenson J.J., Hensley S. 2009. Comparison of Lidar, Radar, and Field Measurements of Canopy Height in Pine and Hardwood Forests of Southeastern North America. Forest Ecology and Management, 257, 1136–1147.

Shtain Z., Filin S. 2011. Accuracy and reliability assessment of GLAS measurements over Israel. Int. Arch. Photogramm. Rem. Sens. Spat. Inf. Sci., 38(5), 247–252.

Simard M., Pinto N., Fisher J.B., Baccini A. 2011. Mapping forest canopy height globally with spaceborne Lidar. J. Geophys. Res., 116.

Simard M., Rivera-Monroy V.H., Mancera-Pineda J.E., Castaneda-Moya E., Twilley R.R. 2008. A Systematic Method for 3D Mapping of Mangrove Forests based on Shuttle Radar Topography Mission Elevation Data, ICESat/GLAS Waveforms and Field Data: Application to Ciénaga Grande De Santa Marta, Colombia. Rem. Sens. Env., 112, 2131–2144.

Su Y., Guo Q. 2014. A practical method for SRTM DEM correction over vegetated mountain areas. ISPRS J. Photogramm. Rem. Sens., 87, 216–228.

Tadono T., Ishida H., Oda F., Naito S., Minakawa K., Iwamoto H. 2014. Precise Global DEM Generation By ALOS PRISM. ISPRS Ann. Photogr. Rem. Sens. Spat. Inf. Sci., II-4, 71–76.

Townshend J.R.G., Carroll M., Dimiceli C., Sohlberg R., Hansen M., DeFries R. 2011. Vegetation Continuous Fields MOD44B, 2001 Percent Tree Cover, Collection 5. University of Maryland, College Park, Maryland, 2001.

Trojanowicz M. 2009. Estimation of an accuracy of global geopotential models EGM96 and EGM08 at lower Silesia Area. Acta Sci. Pol., Geod. Descr. Terr., 8(1).

Tulski S. 2014. Lidar in space. Geodeta, (5) 15–17.

Vassilopoulou S., Hurni L. 2001. The use of digital elevation models in emergency and socio-economic planning: A Case Study at Kos-Yali-Nisyros-Tilos Islands, Greece. Proceedings of 20th International Cartographic Conference, Beijing, China, 3424–3431.

Wilson M., Bates P., Alsdorf D., Forsberg B., Horritt M., Melackm J., Frappart F., Famigieltti J. 2007. Modeling large-scale inundation of Amazonian seasonally flooded wetlands. Geophys. Res. Lett., 34, L15404.

Wright R., Garbeil H., Baloga S.M., Mouginis-Mark P.J. 2006. An assessment of Shuttle Radar Topography Mission digital elevation data for studies of volcano morphology. Rem. Sens. Envir., 105(1), 41–53.

Wylie D., Elronata E., Spinhirne J.D., Palm S.P. 2007. A comparison of Cloud cover statistics from GLAS Lidar with HIRS. J. Climate, 20, 4968–4981.

Zwally H.J., Schutz B., Abdalati W., Abshire J., Bentley C., Brenner A., Bufton J., Dezio J., Hancock D., Harding D., Herring T., Minster B., Quinn K., Palm S., Spinhirne J., Thomas R. 2002. ICESat's laser measurements of polar ice, atmosphere, ocean and land. J. Geodyn., 32, 405–445.

Zwally H.J., Li J., Brenner A.C., Beckley M., Cornejo H.G., DiMarzio J., Giovinetto M.B., Neumann T.A., Robbins J., Saba J.L., Yi D., Wang W. 2011. Greenland ice sheet mass balance: distribution of increased mass loss with climate warming; 2003–07 versus 1992–2002. J. Glac., 57(201), 88–102.

Mgr inż. Sławomir Tulski
Former postgraduate student at
Wrocław University of Environmental and Life Sciences
25 Norwida Street
50-375 Wrocław, Poland
slawomir.tulski@gmail.com
ORCID: 0000-0001-8238-5634

Dr hab. inż. Kazimierz Becek, Univ. Professor
Wrocław University of Science and Technology
Faculty of Geoengineering, Mining and Geology
ul. Na Grobli 15, 50-421 Wrocław
e-mail: kazimierz.becek@pwr.edu.pl
ORCID: 0000-0003-1532-9725